Asian Journal of Chemistry; Vol. 38, No. 6 (2026), 1423-1432
ASIAN JOURNAL OF CHEMISTRY
https://doi.org/10.14233/ajchem.2026.35765

Triazolo-Thiazolidinone Hybrids as Multi-Target Antimicrobial Agents: Synthesis, Docking, ADMET and *in vitro* Validation

TRIVENI SINGIRISETTY[1], K. CHINNA KONDANNA[2], CHAITANYA JINKALA[1], DEVI URUMULA[1], P. GURUSREE[1], JAYASHREE CHINTHA[1] and NARESH BABU CHILAMAKURU[2,*]

[1]Department of Pharmaceutical Chemistry, Raghavendra Institute of Pharmaceutical Education and Research (Autonomous), K.R. Palli Cross, Near SK University, Anantapur-515721, India
[2]Department of Pharmaceutical Analysis, Raghavendra Institute of Pharmaceutical Education and Research (Autonomous), K.R. Palli Cross, Near SK University, Anantapur-515721, India

*Corresponding author: E-mail: nareshbabu.cvn@gmail.com

Received: 9 February 2026 *Accepted*: 14 April 2026 *Published online*: 31 May 2026 AJC-22368

The present study describes one-pot cyclocondensation for the synthesis of a series of novel triazolo-thiazolidinone derivatives (**MC1-MC9**) as potential antimicrobial and antitubercular agents. The synthesised compounds were characterised by their IR, ^{1}H NMR, ^{13}C NMR and mass spectral data. Molecular docking studies against DNA gyrase subunit B of *Staphylococcus aureus* and *Escherichia coli* and lanosterol 14α-demethylase (CYP51), revealed favourable binding affinities and key active-site interactions for several derivatives. ADMET predictions indicated acceptable drug-likeness, pharmacokinetic behaviour and an overall manageable toxicity profile. *In vitro* antimicrobial screening showed dose-dependent activity, with compounds **MC2**, **MC3**, **MC7** and **MC8** exhibiting prominent antibacterial effects, producing zones of inhibition up to 15-16 mm against *S. aureus* and *E. coli* at 200 µg/mL. Antifungal testing against *C. albicans* showed that compounds **MC4** and **MC8** were quite effective, with inhibition zones of 14 mm at 200 µg/mL. Antitubercular screening against *Mycobacterium tuberculosis* H37Rv revealed compounds **MC2** and **MC4** as the most effective compounds at a minimum inhibitory concentration (MIC) of 3.125 µg/mL, although compounds **MC5**, **MC8** and **MC9** had significant action at a MIC of 6.25 µg/mL. The structure–activity relationship analysis revealed that electronic substituents significantly influence biological activity, with **MC2** and **MC4** identified as promising candidates for further optimisation.

Keywords: Triazolo-thiazolidinone, Molecular docking, ADMET, Antibacterial activity, Antifungal activity, Antitubercular activity.

INTRODUCTION

Heterocyclic compounds constitute a fundamental class of pharmacophores in medicinal chemistry, with a significant proportion of approved drugs containing at least one heterocyclic ring. Nitrogen- and sulphur-containing heterocycles are particularly important due to their structural diversity, synthetic accessibility and broad biological activities [1,2]. Among these, 1,2,4-triazole and thiazolidinone scaffolds are recognised as privileged structures exhibiting antibacterial, antifungal, antitubercular, anti-inflammatory and anticancer properties [3-9]. The integration of these two moieties into a single triazolo-thiazolidinone hybrid framework offers the potential for synergistic biological activity along with improved pharmacokinetic characteristics [10-12]. The triazole ring contributes to metabolic stability and facilitates hydrogen bonding and π–π interactions with biological targets, while the thiazolidinone core, containing reactive carbonyl and sulphur functionalities, enables strong interactions with enzyme active sites. These features support their potential to inhibit key microbial enzymes including DNA gyrase and topoisomerase II, making them promising candidates against drug-resistant pathogens [12,13].

To explore multi-target antimicrobial activity, three biologically validated targets were selected: DNA gyrase subunit B from *Staphylococcus aureus* (4P8O) [14] and *Escherichia coli* (5L3J) [15], along with lanosterol 14α-demethylase (CYP51, 3LD6) [16]. DNA gyrase is essential for bacterial DNA replication and supercoiling, and its inhibition leads to cell death; however, rising quinolone resistance necessitates new scaff-

This is an open access journal, and articles are distributed under the terms of the Attribution 4.0 International (CC BY 4.0) License. This license lets others distribute, remix, tweak, and build upon your work, even commercially, as long as they credit the author for the original creation. You must give appropriate credit, provide a link to the license, and indicate if changes were made.

olds targeting the gyrase B subunit. CYP51 plays a key role in fungal ergosterol biosynthesis and its inhibition disrupts membrane integrity. Targeting both enzymes supports a multi-target strategy for developing effective antimicrobial agents.

Advances in the molecular hybridisation and structure-based drug design have facilitated the development of novel heterocyclic systems with enhanced biological profiles. Previous studies [12] have demonstrated that triazolo-thiazolidinone derivatives exhibit promising antimicrobial activity along with favourable ADMET characteristics. In this context, the present study focuses on the design and synthesis of new triazolo-thiazolidinone hybrids, followed by molecular docking, ADMET evaluation and *in vitro* biological assessment, to identify potential multi-target antimicrobial agents effective against resistant bacterial and fungal pathogens.

EXPERIMENTAL

All chemicals and reagents used were of analytical grade and procured from Loba Chemie, HiMedia, Fisher Scientific and Merck. Solvents were purified before use by standard methods. The melting points of synthesised compounds were determined using a Jain melting point apparatus and are uncorrected. Infrared spectra were recorded on a Bruker FTIR spectrophotometer, ^{1}H NMR spectra (Bruker Avance 500 MHz instrument), ^{13}C NMR and mass spectra on a MALDI SYNAPT XS HD spectrometer at SAIF, Panjab University, Chandigarh, India.

Synthetic procedure: A mixture of 4-amino-1,2,4-triazole (**1**) (0.01 mol), substituted aromatic aldehyde (**3**) (0.01 mol) and thioglycolic acid (**2**) (0.01 mol) was refluxed in glacial acetic acid (30-50 mL) in the presence of ammonium acetate (3 g) for 3-4 h. The reaction mixture was continuously stirred under reflux and the progress of the reaction was monitored by thin-layer chromatography (TLC) using solvent system ethyl acetate:*n*-hexane (1:1). Upon completion, the reaction mixture was poured into ice-cold water to precipitate the crude product [17]. The solid was filtered, washed with distilled water and recrystallised from ethanol to obtain pure triazolo-thiazolidinone derivatives (**MC1-MC9**) (**Scheme-I**).

2-(4-Nitrophenyl)-3-(4*H*-1,2,4-triazol-4-yl)-1,3-thiazolidin-4-one (MC1): Yield: 35.03%, m.p. 230-232 ºC, R_f: 0.90; IR (KBr, ν_{max}, cm^{-1}): 1708.99 (C=O), 1515.84, 1345.04 (NO_2), 1422.83 (C–S), 1385.96 (C–N, 3º amine); ^{1}H NMR (500 MHz, DMSO-d_6, δ ppm): 4.35-4.36 (2H, thiazolidinone), 6.93 (1H, thiazolidinone), 7.14-7.64 (4H, m, Ar–H), 8.42 (2H, triazole); ^{13}C NMR (100 MHz, DMSO-d_6, δ ppm): 172.4 (C=O), 153.6, 151.2 (triazole C=N), 147.8 (Ar–C–NO_2), 138.6 (*ipso*-Ar), 129.4, 124.8 (Ar–CH), 66.2 (thiazolidinone –CH), 34.5 (thiazolidinone –CH_2); MS of $C_{11}H_9N_5O_3S$: *m/z* 291.14 [M$^+$].

2-(2-Hydroxyphenyl)-3-(4*H*-1,2,4-triazol-4-yl)-1,3-thiazolidin-4-one (MC2): Yield: 40.59%, m.p. 130-131 ºC, R_f: 0.66; IR (KBr, ν_{max}, cm^{-1}): 3522.15 (O–H), 1704.89 (C=O), 1450.66 (C–S), 1375.56 (C–N, 3º amine); ^{1}H NMR (500 MHz, DMSO-d_6, δ ppm): 3.95 (1H, OH), 4.35-4.39 (2H, s, thiazolidinone –CH_2), 6.98-7.62 (4H, m, Ar–H), 7.78-7.81 (1H, s, thiazolidinone –CH), 8.12–8.15 (2H, s, triazole); ^{13}C NMR (100 MHz, DMSO-d_6, δ ppm): 171.8 (C=O), 154.2, 151.6 (triazole), 156.8 (Ar–C–OH), 136.2 (*ipso*-Ar), 128.7, 124.5, 121.8 (Ar–CH), 65.8 (thiazolidinone –CH), 33.9 (thiazolidinone –CH_2); MS of $C_{11}H_{10}N_4O_2S$: *m/z* 262.13 [M$^+$].

2-(3-Ethoxy-4-hydroxyphenyl)-3-(4*H*-1,2,4-triazol-4-yl)-1,3-thiazolidin-4-one (MC3): Yield: 42.30%, m.p. 135-137 ºC, R_f: 0.78; IR (KBr, ν_{max}, cm^{-1}): 1708.94 (C=O), 1460.82 (C–S), 1333.65 (C–N, 3º amine), 3609.69 (O–H), 1420.92 (R–O–R), 2938.65 (CH_3), 1097.92 (C–O); ^{1}H NMR (500 MHz, DMSO-d_6) δ (ppm): 2.09 (3H, -CH_3), 4.32-4.36 (2H, thiazolidinone), 7.04-7.52 (5H, m, Ar–H), 8.74 (2H, triazole); ^{13}C NMR (100 MHz, DMSO-d_6) δ (ppm): 172.1 (C=O), 153.9, 151.4 (triazole), 154.6 (Ar–C–OH), 146.8 (Ar–C–OEt), 137.4 (*ipso*-Ar), 128.2, 123.9 (Ar–CH), 65.9 (thiazolidinone –CH), 34.2 (thiazolidinone –CH_2), 63.1 (O–CH_2), 14.7 (ethoxy -CH_3); MS of $C_{13}H_{14}N_4O_3S$: *m/z* 306.16 [M$^+$].

2-(4-Chlorophenyl)-3-(4*H*-1,2,4-triazol-4-yl)-1,3-thiazolidin-4-one (MC4): Yield: 79.85%, m.p. 140-142 ºC, R_f: 0.82, IR (KBr, ν_{max}, cm^{-1}): 1712.65 (C=O), 1284.50 (C–S), 1388.71 (C–N, 3º amine), 723.54 (C–Cl); ^{1}H NMR (500 MHz, DMSO-d_6, δ ppm): 5.55 (2H, thiazolidinone), 7.26-7.75 (5H, m, Ar–H), 8.06-8.17 (2H, triazole); ^{13}C NMR (100 MHz, DMSO-d_6, δ ppm): 173.0 (C=O), 152.8, 150.9 (triazole), 139.2 (Ar–C–Cl), 135.4 (*ipso*-Ar), 129.6, 127.4 (Ar–CH), 66.4 (thiazolidinone –CH), 35.1 (thiazolidinone –CH_2); MS of $C_{11}H_9ClN_4OS$: *m/z* 281.06 [M$^+$].

2-(4-Hydroxyphenyl)-3-(4*H*-1,2,4-triazol-4-yl)-1,3-thiazolidin-4-one (MC5): Yield: 43.12%, m.p. 200-201 ºC, R_f: 0.88; IR (KBr, ν_{max}, cm^{-1}): 3361.79 (O–H), 1382.58 (C–N, 3º amine), 1497.01 (C–S); ^{1}H NMR (500 MHz, DMSO-d_6, δ ppm): 3.87-3.90 (2H, thiazolidinone), 6.44-7.27 (5H, m, Ar–H), 7.79-7.81 (2H, triazole); ^{13}C NMR (100 MHz, DMSO-d_6, δ ppm): 171.6 (C=O), 154.5, 151.8 (triazole), 157.3 (Ar–C–OH), 136.8 (*ipso*-Ar), 129.2, 124.1 (Ar–CH), 65.6 (thiazolidinone

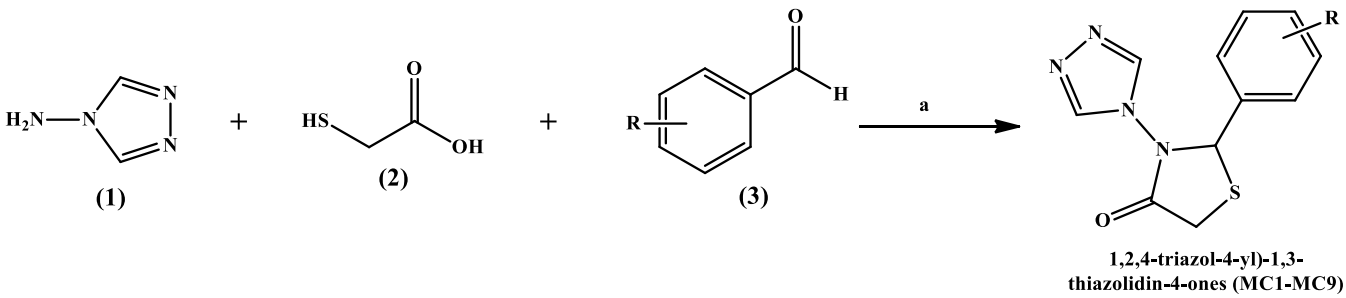

Scheme-I: Reagents and conditions (a) refluxed 70-80 ºC, 03-04 h, ammonium acetate, glacial acetic acid; R = **MC1**; *p*-NO_2; **MC2**; *o*-OH; **MC3**; *p*-OH, *m*-OC_2H_5; **MC4**; *p*-Cl; **MC5**; *p*-OH; **MC6**; *p*-NO_2; **MC7**; *p*-OH, *m*-OCH_3; **MC8**; *p*-OCH_3; **MC9**; *p*-$N(CH_3)_2$

–CH), 33.8 (thiazolidinone –CH_2); MS of $C_{11}H_{10}N_4O_2S$: *m/z* 262.16 [M^+].

2-(3-Nitrophenyl)-3-(4*H*-1,2,4-triazol-4-yl)-1,3-thiazolidin-4-one (MC6): Yield: 47.07%, m.p. 170-172 ºC, R_f: 0.64; IR (KBr, ν_{max}, cm^{-1}): 1735.11 (C=O), 1502.97 (C–S), 1555.57 (NO_2), 1346.15 (C–N, 3º amine); ^{1}H NMR (500 MHz, DMSO-d_6, δ ppm): 3.00-3.05 (2H, thiazolidinone), 3.76 (1H, thiazolidinone), 6.77-7.73 (4H, m, Ar–H), 8.42 (2H, triazole); ^{13}C NMR (100 MHz, DMSO-d_6, δ ppm): 173.4 (C=O), 153.2, 151.0 (triazole), 148.6 (Ar–C–NO_2), 139.5 (ipso-Ar), 130.8, 125.2, 122.6 (Ar–CH), 66.1 (thiazolidinone –CH), 34.7 (thiazolidinone –CH_2); MS of $C_{11}H_9N_5O_3S$: *m/z* 290.99 [M^+].

2-(4-Hydroxy-3-methoxyphenyl)-3-(4*H*-1,2,4-triazol-4-yl)-1,3-thiazolidin-4-one (MC7): Yield: 36.50%, m.p. 155-157 ºC, R_f: 0.75; IR (KBr, ν_{max}, cm^{-1}): 3432.85 (O–H), 1718.68 (C=O), 1458.28 (C–S), 1420.92 (O–CH_3), 1381.41 (C–N, 3º amine), 1016.30 (R–O–R); ^{1}H NMR (500 MHz, DMSO-d_6, δ ppm): 3.86-3.87 (3H, CH_3), 4.16 (2H, thiazolidinone), 7.12-7.87 (5H, m, Ar–H), 9.52-9.53 (2H, triazole); ^{13}C NMR (100 MHz, DMSO-d_6, δ ppm): 172.5 (C=O), 154.0, 151.7 (triazole), 156.4 (Ar–C–OH), 147.2 (Ar–C–OCH_3), 137.1 (*ipso*-Ar), 128.4, 123.7 (Ar–CH), 65.7 (thiazolidinone –CH), 34.1 (thiazolidinone –CH_2), 55.9 (-OCH_3); MS of $C_{12}H_{12}N_4O_3S$: *m/z* 292.30 [M^+].

2-(4-Methoxyphenyl)-3-(4*H*-1,2,4-triazol-4-yl)-1,3-thiazolidin-4-one (MC8): Yield: 38.45%, m.p. 145-147 ºC, R_f: 0.80; IR (KBr, ν_{max}, cm^{-1}): 2932.14 (C–H, OCH_3), 1710.35 (C=O, thiazolidinone), 1462.18 (C–S), 1384.27 (C–N, 3º amine), 1248.62 (Ar–O–CH_3), 1035.48 (C–O); ^{1}H NMR (500 MHz, DMSO-d_6, δ ppm): 3.78 (3H, s, OCH_3), 4.28-4.32 (2H, thiazolidinone –CH_2), 6.92-7.54 (4H, m, Ar–H), 7.85-7.87 (2H, s, triazole); ^{13}C NMR (100 MHz, DMSO-d_6, δ ppm): 172.2 (C=O), 153.5, 151.3 (triazole), 159.2 (Ar–C–OCH_3), 136.6 (*ipso*-Ar), 129.0, 124.6 (Ar–CH), 66.0 (thiazolidinone –CH), 34.3 (thiazolidinone –CH_2), 55.6 (-OCH_3); MS of $C_{12}H_{12}N_4O_2S$: *m/z* 276.14 [M^+].

2-[4-(Dimethylamino)phenyl]-3-(4*H*-1,2,4-triazol-4-yl)-1,3-thiazolidin-4-one (MC9): Yield: 41.72%. m.p. 160-162 ºC, R_f: 0.83; IR (KBr, ν_{max}, cm^{-1}): 2818.44 (N–CH_3), 1706.82 (C=O, thiazolidinone), 1456.91 (C–S), 1387.65 (C–N, 3º amine), 1215.73 (C–N, aromatic amine); ^{1}H NMR (400 MHz, DMSO-d_6, δ ppm): 2.92 (6H, s, N(CH_3)$_2$), 4.24-4.29 (2H, thiazolidinone –CH_2), 6.78–7.46 (4H, m, Ar–H), 7.96-7.98 (2H, s, triazole); ^{13}C NMR (100 MHz, DMSO-d_6, δ ppm): 171.9 (C=O), 153.1, 151.0 (triazole), 151.6 (Ar–C–NMe_2), 136.9 (*ipso*-Ar), 128.6, 123.9 (Ar–CH), 65.8 (thiazolidinone –CH), 34.0 (thiazolidinone –CH_2), 40.3 (-N(CH_3)$_2$); MS of $C_{13}H_{15}N_5OS$: *m/z* 289.18 [M^+].

Molecular docking studies: Molecular docking studies were performed using the Schrödinger Glide software suite (Version 2024-1) to evaluate the binding affinity and interaction profiles of compounds **MC1-MC9** with selected bacterial and fungal target proteins [18,19].

Protein preparation: Crystal structures of *E. coli* DNA gyrase subunit B (PDB ID: 5L3J), *S. aureus* DNA gyrase subunit B (PDB ID: 4P8O) and human lanosterol 14α-demethylase (CYP51, PDB ID: 3LD6) were retrieved from the protein data bank. Proteins were prepared using the protein preparation wizard, involving addition of hydrogens, assignment of bond orders, removal of non-essential water molecules, optimisation of hydrogen-bonding networks and minimisation using the OPLS4 force field. Co-crystallised ligands were used to define the binding site for grid generation. Receptor grids were generated around the active site using Glide's receptor grid generation module. Default van der Waals scaling and partial charge cut-off parameters were applied. In case of 4P8O, conserved water molecules involved in ligand binding were retained during grid preparation.

Ligand preparation: All the synthesised compounds (**MC1-MC9**) were sketched in ChemDraw and imported into Maestro in .mol format. Ligand structures were prepared using LigPrep, which generated low-energy 3D conformations, corrected ionisation states at physiological pH, assigned chirality and minimised energy using the OPLS4 force field.

Molecular docking: Using Glide Standard Precision (SP) mode, prepared ligands were docked onto the generated receptor grids of the prepared proteins. The docking run progressed with several poses for each ligand and the optimum pose for each molecule based on its docking score and important interactions with amino acid residues in the active site was chosen and reported in the results.

ADMET prediction: The *in silico* online tool ADMETlab 2.0 used for evaluation of the ADMET characteristics of the compounds. The generated SMILES notation of each molecule was loaded into the ADMET screening module to check important pharmacokinetic and toxicity characteristics. The tool was used to predict key physico-chemical properties, drug-likeness, absorption and distribution patterns, metabolic stability, elimination pathways and early toxicity profiles. These predictions provide preliminary insight into the pharmacokinetic behaviour, safety and drug-like potential of the designed compounds [20].

Antimicrobial screening: The antimicrobial activity of the synthesised compounds was evaluated against *S. aureus* (MTCC 1430), *E. coli* (MTCC 1610) and *C. albicans* (MTCC 1637) using the cup-and-plate diffusion method in duplicate. Test microorganisms were pre-incubated in peptone broth for 24 h, while sterile nutrient agar was prepared, autoclaved and poured into petri plates. After solidification, microbial cultures were surface-inoculated and wells were aseptically punched into the agar. Each compound was tested at concentrations of 50, 100, 150 and 200 µg/mL and the respective aliquots were introduced into the wells along DMSO as negative (solvent) control. Plates were incubated at 35-37 ºC for 24 h, after which the zones of inhibition were measured to assess antimicrobial potential by comparing with the antibacterial standard ciprofloxacin and antifungal standard griseofulvin [21,22].

Antitubercular activity screening: The minimum inhibitory concentration (MIC) of the test compounds were determined in duplicate at the concentrations 100, 50, 25, 12.5, 6.25, 3.125, 1.56 and 0.78 µg/mL against Mtb H37Rv. The dilution was performed using the 7H9 medium without changing the composition of the medium. The culture suspension was standardised to McFarland and diluted (1:10) to achieve a final inoculum of 1×10^5 cells per well. Rifampicin (1 µg/mL, Sigma-Aldrich) was used as the reference standard, along with culture and solvent (DMSO) controls. Plates were incubated at 37 ºC

for 5 days and examined microscopically for serpentine cord formation. The minimum inhibitory concentration (MIC) was defined as the lowest concentration that completely inhibited visible growth of *M. tuberculosis* [23,24].

RESULTS AND DISCUSSION

The triazolo-thiazolidinone hybrids (**MC1-MC9**) were synthesised *via* a one-pot multicomponent cyclocondensation of 4-amino-1,2,4-triazole, substituted aromatic aldehydes and thioglycolic acid in glacial acetic acid under reflux in the presence of ammonium acetate, as illustrated in **Scheme-I**. The reaction proceeds through initial imine formation followed by intramolecular cyclisation to afford the 1,3-thiazolidin-4-one core, yielding the target compounds in moderate to good yields (35-80%) within 3-4 h. Structural confirmation was achieved using IR, ^{1}H NMR, ^{13}C NMR and mass spectrometry. The IR spectra displayed a characteristic carbonyl (C=O) stretching band around 1735-1700 cm^{-1} along with C–S and C–N vibrations, confirming formation of the thiazolidinone ring, while substituent-specific peaks such as $–NO_2$, –OH, $–OCH_3$ and –Cl verified functional group incorporation. In the ^{1}H NMR spectra, thiazolidinone $–CH_2$ protons appeared around δ 4.2-4.4 ppm and the –CH proton in the δ 6.8-7.8 ppm region, with aromatic protons observed as multiplets and triazole protons appearing as downfield singlets (δ ~7.8-9.5 ppm). The ^{13}C NMR spectra further supported the structures, showing carbonyl carbons around δ 171-173 ppm and triazole C=N signals near δ 150-155 ppm, along with expected aromatic and substituent carbons. Mass spectra exhibited molecular ion peaks consistent with calculated values, confirming molecular integrity. These spectral results confirm the successful synthesis of structurally diverse triazolo-thiazolidinone hybrids, where differences in substituents are likely to modulate electronic characteristics and influence their biological activity.

Molecular docking: The prepared target proteins (PDB IDs: 5L3J, 4P8O and 3LD6) active sites were defined by generating receptor grids around the respective co-crystallised ligands. For 5L3J, the grid was centered at coordinates X = –12.3, Y = 19.77, Z = 22.46 Å; for 4P8O at X = 49.93, Y = –3.83, Z = 18.73 Å; and for 3LD6 at X = 42.47, Y = 4.96, Z = 2.04 Å, each with a grid box dimension of 20 × 20 × 20 Å. The designed compounds, along with standard reference drugs, were docked against all three targets using Glide following the standard extra-precision (XP) protocol. The docking scores (kcal/mol) and binding interactions are summarised in Table-1.

Docking studies on 3LD6 protein revealed that, all the compounds exhibited docking scores in the range of -5.450 to -5.959 indicating stable interactions within the heme-containing active site. Several compounds (**MC1**, **MC4**, **MC6**, **MC8**) interacted directly with HEM 601, suggesting strong affinity towards the catalytic pocket. Compounds **MC3**, **MC5** and **MC7** showed significant interactions with TYR131, while **MC9** displayed binding with PHE139, indicating alternative stabilizing hydrophobic interactions. The reference drug ketoconazole showed the highest affinity (-8.323) compared with the screened compounds. Binding pose of the ketoconazole and compounds **MC9**, **MC4** and **MC8** are shown in Fig. 1.

Docking scores in 4P8O protein were relatively low (-4.35 to -6.05), indicating a smaller binding pocket. The major interaction was seen with GLY85 and ASP81, which are apparently major residues in stabilizing ligands. The docking score was highest in **MC5** (-6.049) having multiple interactions (ASN54, GLY85, ASP81 and THR173), showing a properly aligned binding position. The conventional ciprofloxacin (-4.773) also showed interaction with GLY85 and ASP81, thus validating their importance. The binding position of ciprofloxacin and compounds **MC5**, **MC4** and **MC7** is shown in Fig. 2.

For the 5L3J protein, several compounds **MC2**, **MC5**, **MC7**, **MC8** displayed enhanced affinity (scores ranging from -5.5 to -6.3), with consistent interactions involving ASP73, GLY77 and THR165, highlighting their importance in ligand anchoring. Compounds **MC2** (-6.306) and **MC8** (-6.216) showed the strongest binding among all test molecules. Interactions with ASP49 and ASP73 suggest electrostatic stabilisation within the active site. Ciprofloxacin showed moderate binding (-5.159), but without significant interactions indicating that the synthesised compounds exhibit competitive binding potential for this target. Binding pose of the ciprofloxacin and compounds **MC2**, **MC8** and **MC7** are shown in Fig. 3.

The docking results indicates that several synthesised derivatives exhibit favourable binding energies and significant active-site interactions across all three target proteins, with **MC2**, **MC5**, **MC7** and **MC8** identified as the most pro-

TABLE-1
DOCKING SCORE (kcal/mol) AND INTERACTIONS OF COMPOUNDS (**MC1-MC9**) ON TARGETED PROTEINS

Compound	3LD6 protein		4P8O protein		5L3J protein	
	Docking score	Interactions	Docking score	Interactions	Docking score	Interactions
MC1	-5.618	HEM 601	-4.493	GLY 85, ASP 57	-4.738	ASP 49, GLY 77
MC2	-5.450	HEM 601, GLY 307	-4.810	ASP 81	-6.306	ASP 73
MC3	-5.697	TYR 131	-4.716	ARG 84, GLY 85, ASP 81	-5.942	GLY 77
MC4	-5.834	HEM 601	-5.563	No interactions	-5.876	No interactions
MC5	-5.533	TYR 131	-6.049	ASN 54, GLY 85, ASP 81, THR 173	-5.514	ASP 73, THR 165
MC6	-5.619	HEM 601	-4.493	GLY 85, ASP 57	-4.738	ASP 49, GLY 77
MC7	-5.722	TYR 131	-4.916	GLY 85, ASP 81	-6.084	ASP 73
MC8	-5.727	HEM 601	-4.672	GLY 85	-6.216	No interactions
MC9	-5.959	PHE 139	-4.354	No interactions	-5.458	No interactions
Ketoconazole	-8.323	PHE 139, PHE 234	–	–	–	–
Ciprofloxacin	–	–	-4.773	GLY 85, ASP 81	-5.159	No interactions

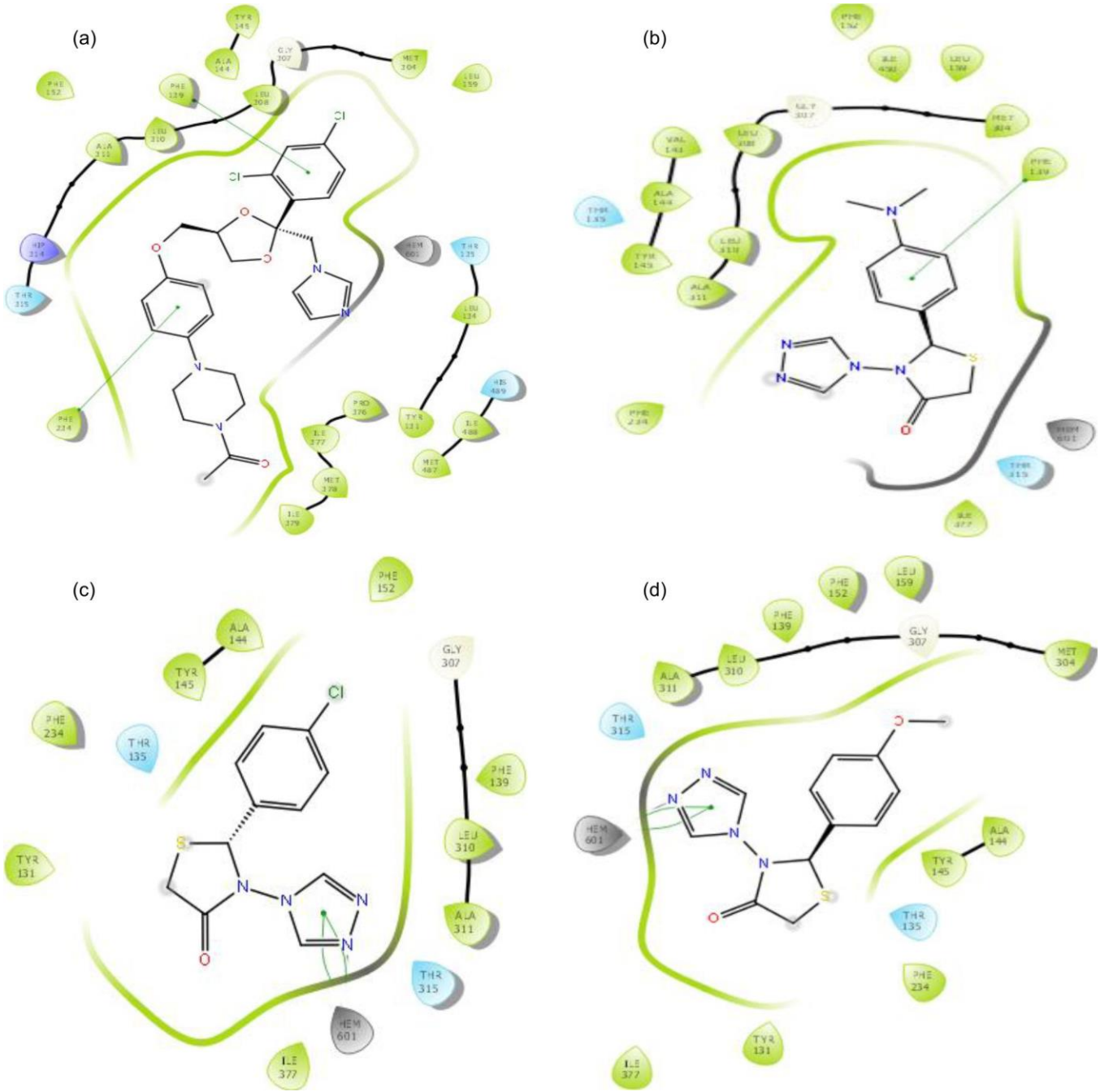

Fig. 1. Binding poses with the 3LD6 protein (a) ketoconazole; (b) **MC9**; (c) **MC4**; (d) **MC8** compounds

mising candidates for further biological evaluation. A heatmap illustrating docking scores and amino acid interaction profiles of the synthesised compounds against the targets is presented in Fig. 4.

ADMET profiling: All the synthesised compounds (**MC1-MC9**) showed physico-chemical profiles that were in line with those of drug-like compounds (Table-2). The molecular weights (262-306 Da) were well within the limits of the Lipinski rule of five and thus indicate good oral bioavailability. The topological polar surface area (TPSA) for all of the compounds was in the range of 51.02 to 94.16 Å^2. This indicates that all of these compounds have good polarity for good solubility and transport across cell membranes. The synthetic accessibility score for all of the compounds was in the range of 3.28 to 3.52. The lipophilicity characteristics (LogP = 0.28-1.80; LogD = 0.85-2.17) show that the compound has a good balance of hydrophilic and lipophilic properties and ideal for good absorption and distribution. All compounds exhibited low to moderate inhibitory effect on key isoenzymes CYP1A2, CYP2C19, CYP2C9, CYP2D6, CYP3A4, it means the metabolic drug-drug interactions are less likely to happen. Compounds **MC4** and **MC8** have somewhat elevated CYP inhibition tendencies and may necessitate more rigorous assessment in subsequent investigations. The clearance (CL = 8.45-12.47 mL/min/kg) and half-life ($T_{1/2}$ = 0.80-0.94 h) results reveal that the metabolism is moderate, which means

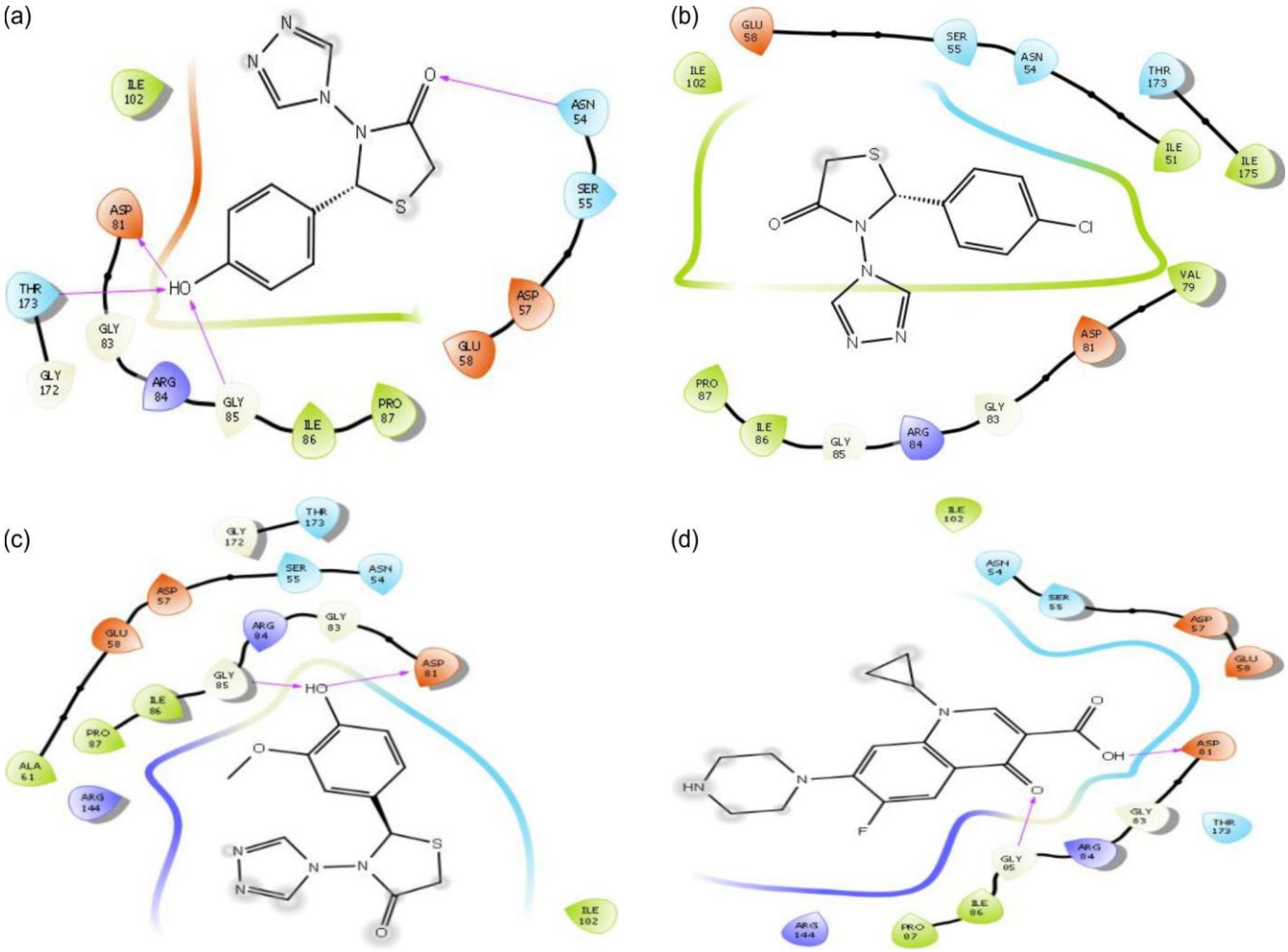

Fig. 2. Binding poses with the 4P8O protein (a) **MC5**; (b) **MC4**; (c) **MC7** compounds; (d) ciprofloxacin

TABLE-2
PHYSICO-CHEMICAL AND ADME PROPERTIES OF SYNTHESISED TRIAZOLO-THIAZOLIDINONE HYBRIDS (**MC1-MC9**)

Compd.	MW	nHA	nHD	TPSA	nROT	Synthetic accessibility score	Lipinski's rule of 5	LogS
MC1	291.04	8	0	94.16	3	3.431	Accepted	-3.12
MC2	262.05	6	1	71.25	2	3.519	Accepted	-2.06
MC3	306.08	7	1	80.48	4	3.458	Accepted	-2.31
MC4	280.02	5	0	51.02	2	3.374	Accepted	-2.92
MC5	262.05	6	1	71.25	2	3.469	Accepted	-2.09
MC6	291.04	8	0	94.16	3	3.472	Accepted	-2.89
MC7	292.06	7	1	80.48	3	3.457	Accepted	-2.12
MC8	276.07	6	0	60.25	3	3.289	Accepted	-2.31
MC9	289.10	6	0	54.26	3	3.432	Accepted	-1.71

Compd.	LogD	LogP	CYP1A2 inh	CYP2C19 Inh	CYP2C9 inh	CYP2D6 inh	CYP3A4 inh	CL	$T_{1/2}$
MC1	1.82	1.13	0.95	0.37	0.25	0.037	0.172	8.451	0.806
MC2	1.00	0.58	0.97	0.17	0.17	0.050	0.126	11.91	0.936
MC3	1.49	0.93	0.98	0.35	0.43	0.04	0.293	11.95	0.901
MC4	2.17	1.80	0.98	0.80	0.38	0.056	0.302	10.12	0.833
MC5	0.89	0.34	0.96	0.19	0.17	0.027	0.096	12.47	0.934
MC6	1.86	1.12	0.97	0.44	0.29	0.049	0.277	8.748	0.859
MC7	0.85	0.28	0.97	0.16	0.22	0.027	0.227	12.33	0.928
MC8	1.41	1.10	0.98	0.64	0.37	0.038	0.353	9.96	0.882
MC9	1.51	1.20	0.98	0.49	0.40	0.022	0.197	9.85	0.900

MW: molecular weight; nHA: number of hydrogen acceptors; nHD: number of hydrogen donors; nROT: number of rotatable bonds

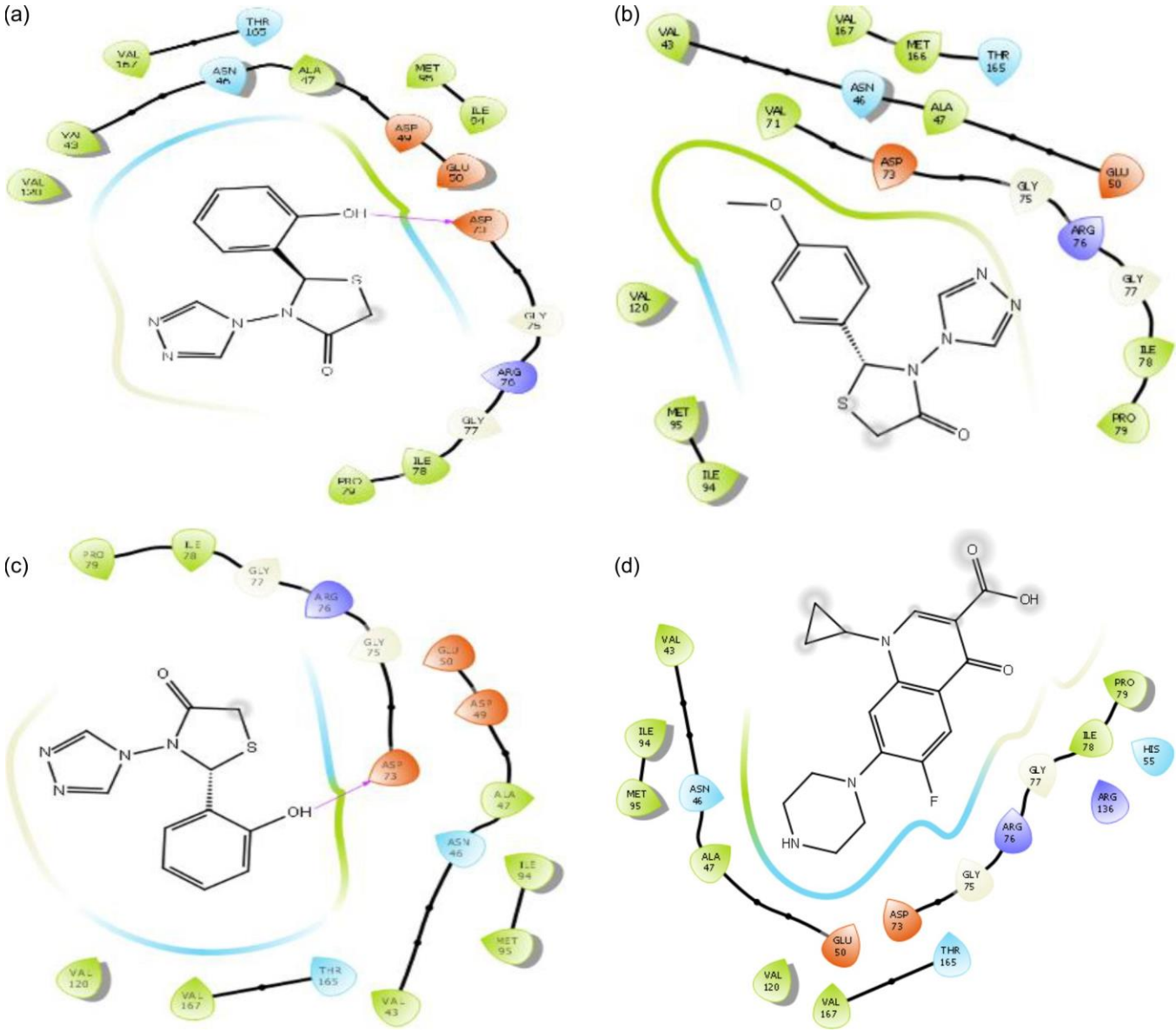

Fig. 3. Binding poses with the 5L3J protein (a) **MC2**; (b) **MC8**; (c) **MC7** compounds; (d) ciprofloxacin

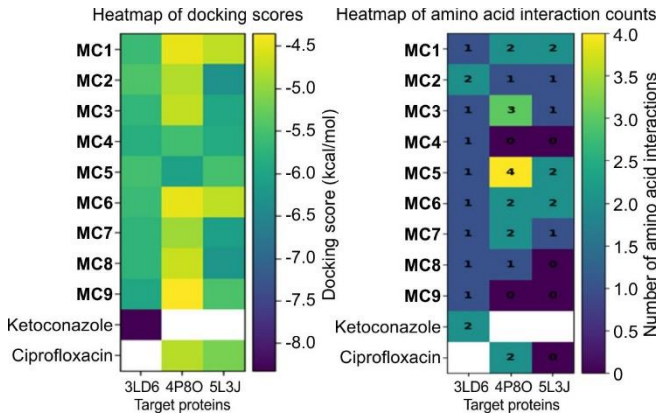

Fig. 4. Heatmap of docking scores and amino acid interaction counts of **MC1**-**MC9** compounds against target proteins

that no chemical has an excessively fast or slow clearance. The toxicity evaluation of the compounds suggests a generally positive safety profile with moderate risks of significant toxicological hazards. The predicted hERG inhibition values for all compounds were low (0.02-0.148), which means that they are less likely to be cardiotoxic (Table-3).

All compounds demonstrated elevated drug-induced liver injury (DILI) scores (0.986-0.990) indicating a potential heaptotoxicity risk frequently associated with heterocyclic scaffolds; this necessitates *in vitro* validation. AME'S mutagenicity predictions indicate that most compounds are non-mutagenic and the risk of skin sensitisation was very low (0.016-0.093), indicates low dermal toxicity. The FDA maximum recommended daily dosage (FDAMDD) values were acceptable for all compounds, which means that the systemic safety margin was good. The chances of cancer and breathing problems were low to moderate for all of the derivatives. The bioconcentration factor (BCF) values were consistently low between 0.327-0.495, which indicates minimal bioaccumulation and long-term toxicity. However, the increased DILI predictions nece-

TABLE-3
TOXICITY PROPERTIES OF SYNTHESISED TRIAZOLO-THIAZOLIDINONE HYBRIDS (**MC1-MC9**)

Compound code	hERG blocker	DILI	ROA	Ame's mutagenicity	Skin sensitization	FDAMDD	EI	Carcino-genicity	Hepato toxicity	Respiratory toxicity	BCF
MC1	0.138	0.989	0.242	0.974	0.822	0.047	0.129	0.956	0.869	0.427	0.355
MC2	0.020	0.988	0.235	0.446	0.797	0.016	0.283	0.945	0.352	0.521	0.395
MC3	0.029	0.987	0.038	0.405	0.278	0.025	0.076	0.964	0.280	0.203	0.483
MC4	0.037	0.990	0.311	0.547	0.765	0.036	0.046	0.955	0.530	0.227	0.495
MC5	0.023	0.989	0.103	0.406	0.687	0.019	0.115	0.959	0.463	0.355	0.338
MC6	0.148	0.988	0.331	0.968	0.806	0.093	0.128	0.955	0.870	0.526	0.360
MC7	0.024	0.986	0.131	0.402	0.347	0.037	0.074	0.962	0.724	0.384	0.414
MC8	0.039	0.989	0.257	0.469	0.631	0.044	0.054	0.966	0.777	0.164	0.414
MC9	0.043	0.989	0.274	0.613	0.760	0.049	0.102	0.962	0.676	0.468	0.327

ssitate targeted *in vitro* hepatotoxicity studies to assess liver safety. Further *in vivo* toxicological investigations and mechanistic evaluations are required to establish long-term safety and exclude potential organ-specific adverse effects.

Antimicrobial results: The synthesised compounds **MC1-MC9** exhibited dose-dependent antibacterial and antifungal activities against *S. aureus* (MTCC 1430), *E. coli* (MTCC 1610) and *C. albicans* (MTCC 1637), as evidenced by the progressive increase in the zone of inhibition from 50 to 200 μg/mL (Table-4). Against *S. aureus*, compounds **MC3**, **MC7**, **MC2** and **MC8** demonstrated notable activity, producing inhibition zones of 15-16 mm at 200 μg/mL, indicating strong efficacy against Gram-positive bacteria. In the case of *E. coli*, compounds **MC2**, **MC4**, **MC5** and **MC7** showed significant activity with similar inhibition zones (15–16 mm at 200 μg/mL), suggesting effective interaction with Gram-negative bacterial membranes. When compared with the reference drug ciprofloxacin (100 μg/mL), which exhibited inhibition zones of 12 mm (*S. aureus*) and 14 mm (E. *coli*), several compounds at higher concentrations (150-200 μg/mL) displayed comparable or enhanced antimicrobial activity.

The synthesised compounds **MC1-MC9** exhibited concentration-dependent antifungal activity against *C. albicans*, with increasing zones of inhibition observed at higher concentrations. Among them, compounds **MC4** and **MC8** showed the highest activity, producing inhibition zones of 14 mm at 200 μg/mL, comparable to the standard drug griseofulvin (10 mm at 100 μg/mL). Compounds **MC3** and **MC9** also demonstrated notable activity with zones of 13 mm at the same concentration, while the remaining compounds showed moderate effects, indicating that specific structural features of compounds **MC4** and **MC8** may enhance their interaction with fungal targets.

The antimicrobial activity data were expressed as mean ± standard deviation (n = 2). A concentration-dependent increase in the zone of inhibition was observed against antimicrobial activity. Statistical analysis revealed low variability (SD < 1.6 mm) indicating good reproducibility. One-way ANOVA demonstrated significant differences ($p < 0.05$) between tested concentrations and compounds confirming the dose-dependent antibacterial efficacy of the synthesised molecules.

Antitubercular activity: The MIC of the synthesised **MC1-MC9** compounds evaluated at 100, 50, 25, 12.5, 6.25, 3.125, 1.56 and 0.78 μg/mL concentrations for their anti-TB activity against Mtb H37Rv and the results are shown in Table-5. From the results of anti-tubercular activity of **MC1-MC9** compounds, the compounds **MC2** and **MC4** exhibited 99.9% of Mtb inhibition at a low MIC of 3.125 μg/mL. Compounds **MC5**, **MC8** and **MC9** compounds showed 99.9% inhibition

TABLE-4
ANTIMICROBIAL ACTIVITY DATA OF SYNTHESISED TRIAZOLO-THIAZOLIDINONE HYBRIDS (**MC1-MC9**)

Compound	Zone of inhibition (mm)											
	Antibacterial activity								Antifungal activity			
	Staphylococcus aureus (Gram-positive)				*Escherichia coli* (Gram-negative)				*Candida albicans*			
	50 μg/mL	100 μg/mL	150 μg/mL	200 μg/mL	50 μg/mL	100 μg/mL	150 μg/mL	200 μg/mL	50 μg/mL	100 μg/mL	150 μg/mL	200 μg/mL
MC1	6	9	11	13	7	10	12	13	6	8	10	11
MC2	9	11	13	15	8	12	14	15	5	7	9	11
MC3	8	11	13	16	8	10	13	14	6	10	11	13
MC4	7	10	12	14	10	13	15	16	7	10	12	14
MC5	7	9	11	13	8	11	13	16	5	7	9	12
MC6	7	10	12	14	6	10	11	13	6	8	10	11
MC7	8	11	14	15	9	12	13	15	6	9	10	12
MC8	9	13	15	16	8	10	12	13	7	10	13	14
MC9	7	9	11	12	6	9	10	12	6	9	11	13
Ciprofloxacin (100 μg/mL)	12				14							
Griseofulvin (100 μg/mL)									10			

TABLE-5
ANTITUBERCULAR ACTIVITY DATA OF SYNTHESISED TRIAZOLO-THIAZOLIDINONE HYBRIDS (**MC1-MC9**)

Compound	MIC (μg/mL) (99.9% of Mtb H37Rv are killed)							
	100	50	25	12.5	6.25	3.125	1.56	0.78
MC1	N/N	N/N	N/N	N/N	P/P	P/P	P/P	P/P
MC2	N/N	N/N	N/N	N/N	N/N	N/N	P/P	P/P
MC3	N/N	N/N	N/N	P/P	P/P	P/P	P/P	P/P
MC4	N/N	N/N	N/N	N/N	N/N	N/N	P/P	P/P
MC5	N/N	N/N	N/N	N/N	N/N	P/P	P/P	P/P
MC6	N/N	N/N	N/N	N/N	P/P	P/P	P/P	P/P
MC7	N/N	N/N	N/N	P/P	P/P	P/P	P/P	P/P
MC8	N/N	N/N	N/N	N/N	N/N	P/P	P/P	P/P
MC9	N/N	N/N	N/N	N/N	N/N	P/P	P/P	P/P
Rifampicin	1 μg/mL							

N/N = No growth of Mtb H37Rv; P/P = Growth of Mtb H37Rv

at 6.25 μg/mL. Moderate activity was observed for compounds **MC1** and **MC6**, which inhibited 99.9% growth at MIC 12.5 μg/mL, whereas compounds **MC3** and **MC7** were comparatively less potent with MIC 25 μg/mL towards Mtb inhibition. These results highlight compounds **MC2** and **MC4** as the most promising candidates at MIC 3.125 μg/mL (Fig. 5).

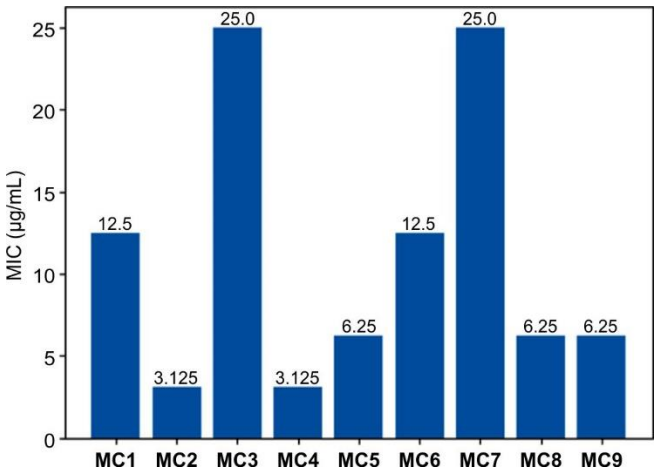

Fig. 5. Anti-TB activity profile of compounds **MC1-MC9** against Mtb H37Rv

Structure–activity relationship (SAR): From the results of molecular docking studies and activity studies of compounds indicates that the nature and position of the substituents present on the phenyl ring attached to the triazolo-thiazolidinone derivatives. Compounds **MC2**, **MC5**, **MC7**, **MC8**, **MC9** containing electron-donating groups such as hydroxyl (-OH), methoxy (-OCH_3) and dimethylamino (-$N(CH_3)_2$) functional groups were found to possess higher antibacterial and antifungal potential due to their enhanced hydrogen bonding ability and permeability. *o*/*p*-Hydroxyl functional groups containing compounds **MC2** and **MC5** were found to exhibited greater anti-TB activity against Mtb H37Rv, this may indicate their ability to interact effectively with the mycobacterial target. The electron-withdrawing functional groups like nitro and chloro functional groups in compounds **MC1**, **MC4**, **MC6** exhibited moderate to good potential. The *p*-chloro functional group in compound **MC4** significantly enhanced the anti-TB potential indicating that increasing the lipophilicity of the drug molecule by attaching appropriate functional groups can lead to enhanced binding affinity towards the target. A balanced combination of lipophilicity and hydrogen-bonding functionality appears critical for enhanced antimycobacterial and antimicrobial activities, highlighting compounds **MC2** and **MC4** as promising lead candidates. Structure–activity relationship analysis suggests that further optimisation could involve introducing both electron-donating groups (*e.g.* –OH, –OCH_3) and lipophilic substituents (*e.g.* –Cl) at appropriate *ortho*/*para* positions on the phenyl ring. Such modifications may simultaneously strengthen hydrogen-bonding interactions and improve lipophilicity, potentially enhancing binding affinity and antimicrobial and antitubercular efficacy.

Conclusion

This study demonstrates that triazolo-thiazolidinone hybrids represent promising antimicrobial agents against bacterial and fungal pathogens, as supported by both *in silico* and *in vitro* investigations. The synthesised compounds **MC1-MC9** were structurally confirmed and exhibited favourable pharmacokinetic properties based on ADMET predictions. Molecular docking studies revealed stable binding and significant interactions with key microbial targets including DNA gyrase subunit B and lanosterol 14α-demethylase, supporting their biological relevance. *In vitro* evaluation showed concentration-dependent antibacterial and antifungal activity within the range of 50-200 μg/mL, with several compounds displaying activity comparable to standard drugs at higher concentrations. Significantly, compounds **MC2** and **MC4** emerged as the most promising antitubercular candidates, exhibiting low MIC values (3.125 μg/mL) against *M. tuberculosis* H37Rv. The SAR analysis indicated that the nature and position of substituents on the phenyl ring significantly influence antimicrobial potency. Further *in vivo* pharmacological and toxicological studies are necessary to confirm the safety and therapeutic potential of these lead compounds, particularly in light of the predicted hepatotoxicity risks.

ACKNOWLEDGEMENTS

The authors are thankful to DST-SERB and DST-FIST Laboratory, Raghavendra Institute of Pharmaceutical Education and Research (RIPER), Anantapur, India for providing the facility for molecular modelling work. The authors are also

thankful to NIRT, Chennai for antitubercular activity and Panjab University for spectral data.

CONFLICT OF INTEREST

The authors declare that there is no conflict of interests regarding the publication of this article.

DECLARATION OF AI-ASSISTED TECHNOLOGIES

During the preparation of this manuscript, the authors used an AI-assisted tool(s) to improve the language. The authors reviewed and edited the content and take full responsibility for the published work.

REFERENCES

1. G. Bérubé, *Expert Opin. Drug Discov.*, **11**, 281 (2016); https://doi.org/10.1517/17460441.2016.1135125
2. Y. Zheng, J. Li, W. Wu, C. Qi and H. Jiang, *Org. Process Res. Dev.*, **28**, 2988 (2024); https://doi.org/10.1021/acs.oprd.4c00186
3. M. Strzelecka and P. Świątek, *Pharmaceuticals*, **14**, 224 (2021); https://doi.org/10.3390/ph14030224
4. J. Sindhu, H. Singh, J.M. Khurana, C. Sharma and K.R. Aneja, *Chinese Chem. Lett.*, **26**, 50 (2015); https://doi.org/10.1016/j.cclet.2014.09.006
5. N.D. Rode, A.D. Sonawane, L. Nawale, V.M. Khedkar, R.A. Joshi, A.P. Likhite, D. Sarkar and R.R. Joshi, *Chem. Biol. Drug Des.*, **90**, 1206 (2017); https://doi.org/10.1111/cbdd.13040
6. J. Hu, Y. Wang, X. Wei, X. Wu, G. Chen, G. Cao, X. Shen, X. Zhang, Q. Tang, G. Liang and X. Li, *Eur. J. Med. Chem.*, **64**, 292 (2013); https://doi.org/10.1016/j.ejmech.2013.04.010
7. O. Gupta, T. Pradhan and G. Chawla, *J. Mol. Struct.*, **1274**, 134487 (2023); https://doi.org/10.1016/j.molstruc.2022.134487
8. N.B. Chilamakuru, *Asian J. Pharm. Clin. Res.*, **6**, 29 (2013).
9. I.A. Gad El-Karim, M.S. Amine, A.A. Mahmoud and A.S. Gouda, *J. Surfactants Deterg.*, **17**, 509 (2014); https://doi.org/10.1007/s11743-013-1530-9
10. S. Maddela, G.E. Mathew, D.G. Parambi, F. Aljoufi and B. Mathew, *Lett. Drug Des. Discov.*, **16**, 220 (2018); https://doi.org/10.2174/1570180815666180516102100
11. D.S. Reddy, M. Kongot and A. Kumar, *Tuberculosis*, **127**, 102050 (2021); https://doi.org/10.1016/j.tube.2020.102050
12. F.A. Nashaan and M.S. Al-Rawi, *Chem. Methodol.*, **7**, 106 (2023); https://doi.org/10.22034/CHEMM.2023.362512.1610
13. B. Dwivedi, D. Bhardwaj and D. Choudhary, *RSC Adv.*, **14**, 8341 (2024); https://doi.org/10.1039/D4RA00990H
14. A.-L. Grillot, A.L. Tiran, D. Shannon, E. Krueger, Y. Liao, H. O'Dowd, Q. Tang, S. Ronkin, T. Wang, N. Waal, P. Li, D. Lauffer, E. Sizensky, J. Tanoury, E. Perola, T.H. Grossman, T. Doyle, B. Hanzelka, S. Jones, V. Dixit, N. Ewing, S. Liao, B. Boucher, M. Jacobs, Y. Bennani and P.S. Charifson, *J. Med. Chem.*, **57**, 8792 (2014); https://doi.org/10.1021/jm500563g
15. M. Gjorgjieva, T. Tomasic, M. Barancokova, S. Katsamakas, J. Ilas, P. Tammela, L. Peterlin Mašič and D. Kikelj, *J. Med. Chem.*, **59**, 8941 (2016); https://doi.org/10.1021/acs.jmedchem.6b00864
16. N. Strushkevich, S.A. Usanov and H.-W. Park, *J. Mol. Biol.*, **397**, 1067 (2010); https://doi.org/10.1016/j.jmb.2010.01.075
17. M.T. Ubeid, H.K. Thabet and S.A. El-Feky, *Heterocycl. Commun.*, **22**, 43 (2016); https://doi.org/10.1515/hc-2015-0135
18. N.B. Chilamakuru, A.D. Vn, N. Pallaprolu, A. Dande, D. Nair, R.V. Pemmadi and R. Peraman, *Eur. J. Med. Chem.*, **272**, 116479 (2024); https://doi.org/10.1016/j.ejmech.2024.116479
19. N.B. Chilamakuru, T. Singirisetty, A. Bodapati, S.D.M. Kallam, V.K. Nelson, P.R. Suryadevara and S. Thangaswamy, *Luminescence*, **39**, e70026 (2024); https://doi.org/10.1002/bio.70026
20. G. Xiong, Z. Wu, J. Yi, L. Fu, Z. Yang, C. Hsieh, M. Yin, X. Zeng, C. Wu, A. Lu, X. Chen, T. Hou and D. Cao, *Nucleic Acids Res.*, **49(W1)**, W5 (2021); https://doi.org/10.1093/nar/gkab255
21. B. Aneja, M. Azam, S. Alam, A. Perwez, R. Maguire, U. Yadava, K. Kavanagh, C.G. Daniliuc, M.M.A. Rizvi, Q.M.R. Haq and M. Abid, *ACS Omega*, **3**, 6912 (2018); https://doi.org/10.1021/acsomega.8b00582
22. C. Babu, S. Triveni, M. Jyothi, B. Yamuna and A. Yamini, *Asian J. Chem.*, **32**, 2753 (2020); https://doi.org/10.14233/ajchem.2020.22821
23. V.B. Makane, V.S. Krishna, E.V. Krishna, M. Shukla, B. Mahizhaveni, S. Misra, S. Chopra, D. Sriram, V.A. Dusthackeer and H.B. Rode, *Eur. J. Med. Chem.*, **164**, 665 (2019); https://doi.org/10.1016/j.ejmech.2019.01.002
24. J.-C. Palomino, A. Martin, M. Camacho, H. Guerra, J. Swings and F. Portaels, *Antimicrob. Agents Chemother.*, **46**, 2720 (2002); https://doi.org/10.1128/AAC.46.8.2720-2722.2002